

An improved algorithm for the numerical simulation of cyclic voltammetric curves affected by the ohmic potential drops and its application to the kinetics of bis(biphenyl)chromium(I) electroreduction

Marek Orlik *

Laboratory of Electroanalytical Chemistry, Department of Chemistry, University of Warsaw, ul. Pasteura 1, PL-02-093 Warsaw, Poland

Received 15 July 2004; received in revised form 27 September 2004; accepted 4 October 2004

Available online 11 November 2004

Abstract

Previously published algorithms for the modeling of cyclic voltammetric curves affected by ohmic potential drops, in terms of the classical explicit finite differences method, are discussed briefly. A fast and efficient numerical procedure suitable for such simulations is described. This approach exhibits high numerical stability for both high scan rates and large uncompensated ohmic resistances. The procedure is based on the calculation of the faradaic current as a root of the non-linear equation, with a simultaneous calculation of the capacitive current. Comparison of the cyclic voltammograms obtained using this method with those calculated using alternative published procedures proves its validity. For comparison with the experimental data, the cyclic voltammetric response for the reduction of bis(biphenyl)chromium(I) tetraphenylborate in *N,N*-dimethylformamide is shown and the kinetic parameters of this process are fitted. Compared to earlier modelings, they show better concordance with the results of studies at microelectrodes. In conjunction with earlier successful applications of the analogous numerical procedure to the realistic modeling of electrochemical oscillations and multistability at a constant external voltage, the algorithm presented appears to be one of the most applicable methods of calculation of the electrochemical responses affected by the ohmic potential drops.

© 2004 Elsevier B.V. All rights reserved.

Keywords: Cyclic voltammetry; Ohmic drops; Digital simulation; Bis(biphenyl)chromium(I) reduction

1. Introduction

This short paper has been inspired by the discussion on various published algorithms for the digital simulation of cyclic voltammetric curves affected by the uncompensated ohmic potentials drops. In such a case, the electrode potential effective for the interfacial charge transfer reaction E differs from the externally applied voltage U :

$$E = U - (I_f + I_c)R_u, \quad (1)$$

where R_u is the (uncompensated) serial resistance in a typical $R_u(Z_f C_d)$ equivalent circuit, where I_f and I_c denote the faradaic and the capacitive current, respectively. The main source of the calculation problems is the difference between the externally imposed linear voltage scan rate $dU/dt = \text{const.}$ and the resulting non-linear scan rate dE/dt

$$\frac{dE}{dt} = \frac{dU}{dt} - R_u \frac{d(I_f + I_c)}{dt}. \quad (2)$$

The problem of a strict calculation of the $I-U$ response in such a case has been solved in several ways, including, among others, the numerical integration of the appropriate integral equation [1–4] and typical

* Tel.: +48 22 822 02 11x245; fax: +48 22 822 59 96.

E-mail address: morlik@chem.uw.edu.pl.

methods of digital simulation of the electrode processes [5–8] for the integration of Fick's diffusion equations. In turn, for the solutions based solely on a digital simulation, two different approaches can be distinguished, in which either the currents are calculated iteratively for a given potential [5–7] or the explicit, non-iterative calculation of the faradaic current is coupled with the calculation of the capacitive current, charging the electrode to the actual potential E [8] (a similar approach was used earlier by Rosenmund and Doblhofer [9] for the simulation of the chronoamperometric experiment with the emission of electrochemiluminescence).

There are two aims of this paper: (i) a brief analysis of the validity of the earlier approach [7] for the simulation of realistic fast-scan cyclic voltammograms in the presence of large ohmic drops – in view of the discussion included in [8]; (ii) a description of the optimized version of the algorithm from [7].

2. Comparison of different algorithms for the simulation of cyclic voltammetric curves

Of course, theoretically, for the same input parameters of the model system, all the methods of calculations should yield practically identical voltammetric curves. It is thus interesting that a recent discussion [8] suggested that the algorithm published in [7] could produce cathodic–anodic peak separations somewhat different from those of the other published approaches. However, careful comparison of the model conditions corresponding to the simulations described in [7,8] shows clearly that a few mV discrepancy in the peak separations, *apparently* produced by the procedure from [7] was a result of the following misunderstanding: in [7] the peak separations for the *multicyclic* voltammetric experiments (more precisely – for the 3rd negative–positive cycle)

were modeled, whereas in [8] the peak potentials were calculated only for the *first* negative–positive cycle. The peak separations obtained for the same first cycle were very close to each other for both approaches, as the exemplary data sets in Table 1 (cf. columns (a)–(c)) prove. The conclusion is thus that all the algorithms published so far yield practically the same calculation results, so all of them are essentially correct. Furthermore, the algorithm published in [7] has, for the last several years, been successfully applied to the kinetic analysis of bis(biphenyl)chromium(I) electroreduction in *N,N*-dimethylformamide [7], for Eu^{3+} electroreduction in *N,N*-dimethylformamide [10] and dimethylsulfoxide in various supporting electrolytes [11–13]. Nevertheless, one should admit here that the approach of Deng and Lin [8] definitely ensures a shorter computation time and, in a more natural way than the method given in [7], generates the effect of the non-zero cell time constant ($R_u C_d$) on the shape of cyclic voltammograms. Also the numerical stability of calculations proposed in [7] appeared unsatisfactory for the combination of relatively high ohmic potential drops and high scan rates. In view of the latter conclusions, it became clear that the iterative algorithm published in [7] required an optimization.

Over the last few years, we have been working on the realistic modeling of the electrochemical non-linear phenomena (i.e. oscillations and multistabilities) appearing in systems with negative differential resistance (NDR) in their current–potential characteristics. Such systems also require sufficient (then even intentionally introduced) ohmic potential drops for the destabilization of the trivial single steady-state toward more complex dynamic behavior. Particularly if oscillations are induced, the sharp variations of the faradaic and capacitive currents require a high numerical stability of the simulation procedure, if such physical instabilities are to be modeled successfully. Thus, it also became evident that the algo-

Table 1

Comparison of the cathodic–anodic peak separations ΔE_p for the *first* cycle of the voltammetric curves, simulated for the same input parameters using different numerical approaches^a

v (V s^{-1})	ΔE_p (mV)			ΔE_p (c) – ΔE_p (a) (mV)	ΔE_p (mV)	ΔE_p (d) – ΔE_p (a) (mV)
	a	b	c			
1111.1	652.00	652.0	652.27	0.27	652.27	0.27
625.0	485.75	485.5	485.87	0.12	485.87	0.12
400.0	395.00	395.0	394.67	–0.33	395.20	0.20
204.1	297.25	298.0	297.07	–0.18	297.07	–0.18
100.0	226.0	226.5	226.13	0.13	226.67	0.67

(a) Numerical calculation using approach by Andrieux et. al. (data taken from [8]). (b) Digital simulation by Deng and Lin (data taken from [8]). (c) This work – digital simulation according to Orlik [7] for *single-scan* cyclic voltammetry. (d) This work – digital simulation according to the present algorithm for *single-scan* cyclic voltammetry.

Parameters of simulation for (c,d): number of time intervals in single scan $N = 1500$, dimensionless diffusion coefficient, $\beta = D\Delta t/(\Delta x)^2 = 0.45$.

^a Formal potential (E_f^0): -1.1 V, diffusion coefficient $D_{\text{ox}} = D_{\text{red}} = 5 \times 10^{-6}$ $\text{cm}^2 \text{s}^{-1}$, bulk reactant concentrations: $c_{\text{ox}}^0 = 1 \times 10^{-3}$ mol dm^{-3} , $c_{\text{red}}^0 = 0$, number of electrons $n = 1$, transfer coefficients $\alpha_{\text{c}} n = \alpha_{\text{a}} n = 0.5$, standard heterogeneous rate constant $k_s = 0.5$ cm s^{-1} , electrode area $A = 1.38 \times 10^{-2}$ cm^2 , double layer capacitance $C_d = 0.1173$ μF (8.5 $\mu\text{F cm}^{-2}$), uncompensated solution resistance $R_u = 800$ Ω , scan potential range: -0.7 to -1.5 V.

rithm essentially based on the same principles as described in [7] did not ensure sufficient numerical stability. Also, the effect of the cell time constant had to be implemented in an explicit numerical way to the simulation program, for reproduction of the instantaneous variations of the coupled faradaic and capacitive currents.

In an attempt to optimize the algorithm from [7] to such calculations it appeared that an appropriate rearrangement and combination of the key equations for the faradaic and capacitive currents would lead to a numerically highly stable and fast calculation procedure for the modeling of oscillations [14,15], as well as bistability [16] in the electroreduction of Ni(II)-SCN⁻ complexes, for the conditions when the externally applied voltage U was fixed. It was thus a natural consequence to check how this modified algorithm would work after its adaptation to the simulation of the potentiodynamic, cyclic voltammetric curves in the presence of ohmic potential drops.

3. Construction of the numerical algorithm for the modeling of CV curves

The model electrode process $\text{Ox} + ne = \text{Red}$ will be considered. The simplest explicit finite numerical method (in the so-called box variant [17] with the uniform space grid) served as the basis for the derivation of the difference equations of transport. The space coordinate in the solution was divided into equal intervals Δx and

$$I_c(j) = C_d \frac{dE}{dt} \cong C_d \frac{E(j) - E(j-1)}{\Delta t}, \quad (3)$$

$$I_f(j) = nFAf_{\text{ox}}(0, j), \quad (4)$$

with the flux of the reactant Ox at the electrode surface

$$f_{\text{ox}}(0, j) = -\frac{c_{\text{ox}}(1, j)k_f - c_{\text{red}}(1, j)k_b}{1 + \left[\frac{k_f(j)}{2D_{\text{ox}}} + \frac{k_b(j)}{2D_{\text{red}}} \right] \Delta x}, \quad (5)$$

and the rate constants of the reduction and oxidation, respectively:

$$k_f(j) = k_s \exp[-\alpha_c n(F/RT)(E(j) - E_f^0)], \quad (6)$$

$$k_b(j) = k_s \exp[\alpha_a n(F/RT)(E(j) - E_f^0)]. \quad (7)$$

The cell time constant was then introduced into the numerical model in the form of the appropriate analytical expressions [7].

In the present modification of that procedure, the following changes in the original procedure [7] were made. The difference expression for the capacitive current (3) was combined with Eq. (1), yielding the expression,

$$I_c(j) = C_d \frac{U(j) - [I_c(j) + I_f(j)]R_u - E(j-1)}{\Delta t}, \quad (8)$$

which was rearranged to the form:

$$I_c(j) = C_d \frac{U(j) - I_f(j)R_u - E(j-1)}{\Delta t + R_u C_d}. \quad (9)$$

The latter expression was substituted for $I_c(j)$ in the equation for the faradaic current:

$$I_f(j) = -nFA \times \frac{c_{\text{ox}}(1, j)k_s \exp\{-(\alpha_c n)[U - [I_f(j) + I_c(j)]R_u - E_f^0]/RT\} - c_{\text{red}}(1, j)k_s \exp\{(\alpha_a n)[U - [I_f(j) + I_c(j)]R_u - E_f^0]/RT\}}{1 + \left[\frac{k_s \exp\{-(\alpha_c n)[U - [I_f(j) + I_c(j)]R_u - E_f^0]/RT\}}{2D_{\text{ox}}} + \frac{k_s \exp\{(\alpha_a n)[U - [I_f(j) + I_c(j)]R_u - E_f^0]/RT\}}{2D_{\text{red}}} \right] \Delta x}. \quad (10)$$

the time coordinate – into equal time intervals Δt , meeting the stability condition $\beta = D\Delta t/(\Delta x)^2 \leq 0.5$. The subsequent spatial steps are enumerated with the $i = 1, \dots, M$ index, and the time steps with the $j = 1, \dots, N$ index. Thus the concentration of the given reactant (Ox or Red) is denoted by $c(x, t) \equiv c(i, j)$. For the calculations of the progress of the transport of Ox and Red species in the solution, the spherical symmetry of diffusion was assumed, in order to enable strict comparison of the simulation results with the experimental data acquired for the hanging mercury drop electrode.

In the formerly published procedure [7] the capacitive and the faradaic currents were determined numerically as the two roots of the system of the following equations:

The numerical procedure for calculation of I_f and I_c is realized as follows for the conditions of the voltage scan. For $t = 0$ the capacitive current is set to zero and the electrode potential $E(0) = U(0)$. For given $U(j)$, based on $E(j-1)$, the faradaic current $I_f(j)$ is calculated as a root of Eq. (10), preferably with the always convergent bisection method (or Müller's method as its particularly efficient modification [18]). Two first approximations of this current are required, which can be taken as e.g. the limits of the interval $[0, I_p]$ where I_p is the peak current for the reversible system, given by the Randles-Ševčík equation [19,20], or this full interval can be conveniently compressed to an appropriately smaller subinterval. The capacitive current $I_c(j)$ is calculated simultaneously with $I_f(j)$, from Eq. (9).

In this way, instead of the system of two Eqs. (3) and (4) only a single non-linear equation (10) is obtained, with I_f being thus the only root to determine iteratively. One should emphasize that although, from the point of view of the formal mathematics, the above approach may seem to be equivalent to the previous one [7], the *numerical* behavior of the iterative procedure based on a single equation (10) is much more satisfactory than that described in [7], also because it explicitly generates the effect of the cell time constant.

To summarize, application of the above-modified algorithm to the simulation of the cyclic voltammograms had the following main advantages:

- (i) calculations of the CV curves were significantly faster, reaching a speed comparable to that of the non-iterative approach recommended by Deng and Lin [8] (see also the caption to Fig. 2 for the comparison of the computation times as an example);
- (ii) the effect of the cell time constant was simulated fully numerically, without any artificial implementation of the analytical relationships to the simulation model
- (iii) numerous tests showed that the numerical stability of the calculations was strongly improved, which allowed the simulation of cyclic voltammograms for much higher ohmic resistances and higher scan rates than previously [7].

Fig. 1 shows the cyclic voltammograms simulated with the above modified numerical procedure as an example.

Fig. 2 shows that the curves simulated with the algorithm presented here and with the algorithm of Deng and Lin [8] for the same input parameters, are practically indistinguishable. Results of additional comparative calculations with these algorithms, shown as the cathodic–anodic peak separations, are given also in the two last columns of Table 1.

Fig. 3 compares the course of the capacitive current simulated with the above algorithm for the case when the electroactive species is absent, with the current calculated from the analytical relationships:

$$I_c = \text{sgn}(v) \cdot C_d |v| \cdot f(t, \tau), \quad (11)$$

with:

$$\tau = R_u C_d, \quad (12)$$

$$f(t, \tau) = \begin{cases} 1 - \exp(-t/\tau), & \text{for the first half - cycle} \\ 1 - 2 \exp\{-[t - (N_{1/2} - 1)T_{1/2}]/\tau\}, & \text{for the following half - cycles,} \end{cases} \quad (13)$$

where t is the actual time of the voltammetric experiment, $T_{1/2}$ is the duration time of every half-cycle and

$N_{1/2}$ is the number of the actual half-cycle. The signum factor $\text{sgn}(v)$ controls the sign of the current, depending of the direction of the scan, e.g. for the negative scan $\text{sgn}(v) = \text{sgn}(dU/dt) = -1$.

Finally, the algorithm discussed was used here for the model reproduction of the cyclic voltammetric curve for bis(biphenyl)chromium(I) tetraphenylborate reduction in a 0.1 mol dm^{-3} solution of tetrabutylammonium perchlorate in *N,N*-dimethylformamide. In this paper, a new set of experimental data recorded at the HMDE was used. The experimental procedure for this measurement, made in a two-electrode system, was described in [7]. More details are given in the caption to Fig. 4 which shows the comparison of the experimental and the simulated CV curves for the BCr(I)/(0) redox couple. The fitted apparent standard rate constant should be consid-

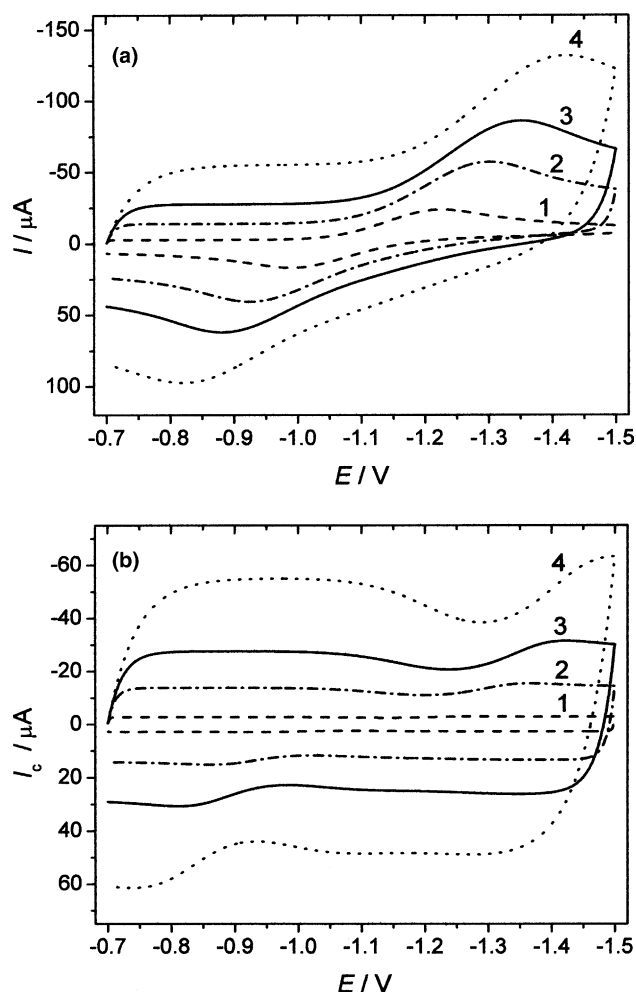


Fig. 1. (a) Exemplary cyclic voltammograms (the first negative-positive cycles) at the spherical electrode, simulated for the scan rates v : (1) 10; (2) 50; (3) 100; (4) 200 V s^{-1} and the following common parameters: $D_{\text{ox}} = D_{\text{red}} = 5 \times 10^{-6} \text{ cm}^2 \text{ s}^{-1}$, $c_{\text{ox}}^0 = 1 \times 10^{-3} \text{ mol dm}^{-3}$, $c_{\text{red}}^0 = 0$, $n = 1$, $\alpha_c = \alpha_a = 0.5$, $k_s = 0.01 \text{ cm s}^{-1}$, $E_f^0 = -1.1 \text{ V}$, $A = 1.38 \times 10^{-2} \text{ cm}^2$, $R_u = 800 \text{ } \Omega$, $C_d = 0.276 \text{ } \mu\text{F}$. (b) The isolated contributions from the capacitive current to the corresponding curves from Part (a).

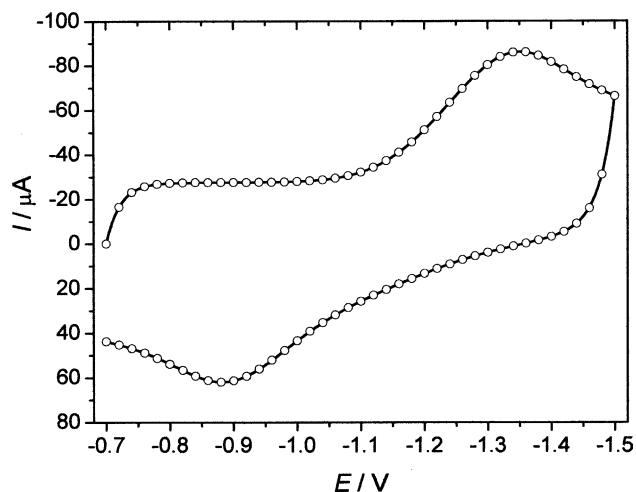


Fig. 2. Comparison of the cyclic voltammogram represented by curve 3 in Fig. 1-(a) (—) (computation time = 0.75 s) with the voltammogram simulated for the same input parameters using the algorithm by Deng and Lin [8] (○) (computation time = 0.66 s). In the numerical model the uniform spatial grid was used for the discretization scheme. The procedure was written in Turbo Pascal 7.0 and run on a Pentium III machine.

ered a lower limit for the true value since for larger values of k_s^{app} the changes in the simulated voltammogram are only subtle. Even this lower limit is however, significantly higher than the value of k_s^{app} determined previously (0.12–0.15 cm s^{-1}) [7] from another data set analyzed only in terms of the cathodic–anodic peak separations, instead of fitting of the entire voltammogram. It is noteworthy that the presently estimated k_s^{app} thus becomes closer to that obtained for the same system using hemispherical submicroelectrodes ($0.50 \pm 0.08 \text{ cm s}^{-1}$) [7,21].

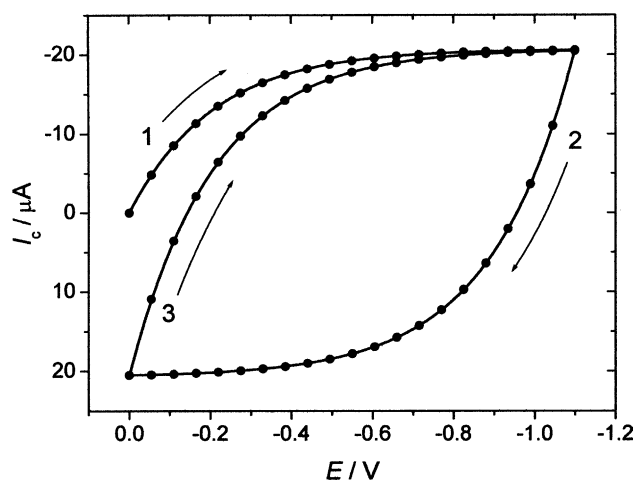


Fig. 3. Capacitive current, simulated (●) and calculated from Eqs. (11)–(13) (—) for the first (1) and the following (2,3) half-cycles of multicyclic voltammetry, in the absence of the electroactive species. Parameters: $R_u = 10 \text{ k}\Omega$, $C_d = 0.207 \text{ }\mu\text{F}$, $A = 1.38 \times 10^{-2} \text{ cm}^2$, $v = 100 \text{ V s}^{-1}$.

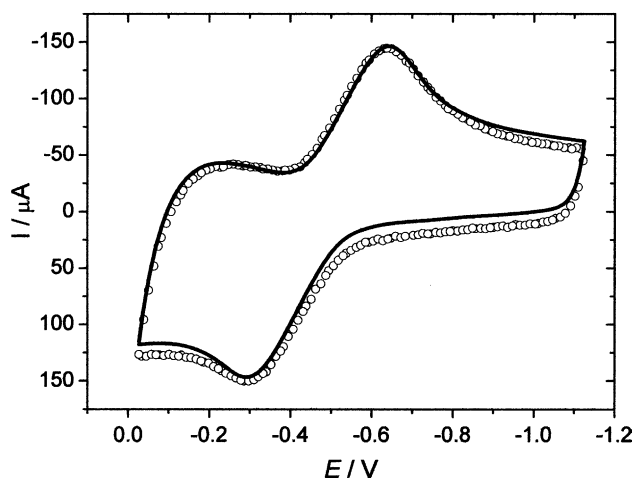


Fig. 4. Comparison of the experimental (○) and simulated (—) multicyclic voltammograms for the electrode process of $1.058 \times 10^{-3} \text{ mol dm}^{-3}$ bis(biphenyl)chromium(I) tetraphenylborate in 0.1 mol dm^{-3} TBAP in N,N -dimethylformamide (DMF). The two-electrode arrangement: hanging mercury drop electrode (HMDE, $A = 1.38 \times 10^2 \text{ cm}^2$) – mercury pool ($A = 12 \text{ cm}^2$) was applied, with the inter-electrode distance $d = 2 \text{ mm}$, and the inter-electrode solution resistance $R_u = 680 \text{ }\Omega$. The scan rate $v = 400 \text{ V s}^{-1}$. The potential scale is expressed vs. the mercury pool which was more negative by 645 mV than the potential of the $\text{Ag|0.01 mol dm}^{-3} \text{ Ag}^+ + 0.1 \text{ mol dm}^{-3} \text{ TBAP}$ (DMF) reference cell. Potential-dependent double layer capacitances were used [10] and implemented to the model via the spline interpolation. Parameters of the model: $E_r^0 = -0.471 \text{ V}$, $D_{\text{ox}} = D_{\text{red}} = 4.44 \times 10^{-6} \text{ cm}^2 \text{ s}^{-1}$ [21], $k_s^{\text{app}} = 0.6 \text{ cm s}^{-1}$, $\alpha_c = \alpha_a = 0.5$. Results of the fifth voltammetric cycles are shown.

4. Conclusions

The first main conclusion is that the modified iterative calculation of the I – E dependence is in better accord with the algorithm described by Deng and Lin [8] than the earlier approach [7]. In conjunction with earlier successful modelings of transient oscillations [14,15] and true steady-states comprising the multistable regions [16], one may conclude that an efficient, highly stable and quite universal algorithm was described here. It seems that, aside from cyclic voltammetry, this algorithm is particularly useful for the modelling of multistability, when, for a given external voltage U , more than one steady-state current can flow. The total interval of physically reliable currents $[0, I_{\text{max}}]$ is then divided into a necessary number N of subintervals $\Delta I = I_{\text{max}}/N$ and in every such subinterval the faradaic current as the root is searched for, using the always convergent bisection method. Then one can be sure that all the physically reliable roots, independently of their physical stability, i.e. both stable and unstable steady-state faradaic currents, will be found.

One should add that, compared to very recent developments in the numerical simulation of complex electrode processes (cf. e.g. [22,23]), it is not the aim of the present paper to compete with the approaches that

also involve migrational transport and double layer effects, and which therefore usually require a mathematically much more sophisticated approach based on implicit techniques. However, even compared to such achievements, the following advantages of the approach presented above can still be considered as a second main conclusion of this paper: (i) relative mathematical simplicity; (ii) successful application to a variety of electrochemical problems, also beyond cyclic voltammetry; (iii) quite a high stability of calculations. The latter conclusion follows not only from the analysis of the above-given calculations, but is additionally confirmed by successful, similar (explicit finite differences) computations of the faradaic current controlled by the ohmic drops in the thin-layer cell, performed for the following, quite demanding conditions: the solution electroneutrality is not attained and, beside diffusion, not only migration [24], but also coupled convection modeled with the Navier–Stokes equation [25] has to be involved in the transport of both the electroactive species and the supporting electrolyte. Thus, in spite of more advanced mathematical treatments, which may offer quite a high stability and accuracy of calculations, and which evidently are the future of the most efficient simulation techniques in electrochemistry (but at the cost of the simplicity of algorithms), the conventional explicit finite-differences method still remains a valuable and efficient approach.

The final conclusion is that, in the opinion of the author, the present communication ends the debate on the modeling of cyclic voltammetric curves, arising from the work in [7,8].

Acknowledgements

The author is greatly indebted to Prof. Gerhard Gritzner for helpful discussions. Financial support from the Johannes Kepler Universität Linz (Austria), where

the experimental data were collected, is gratefully acknowledged.

References

- [1] J.C. Imbeaux, J.M. Savéant, *J. Electroanal. Chem.* 28 (1970) 325.
- [2] J.C. Imbeaux, J.M. Savéant, *J. Electroanal. Chem.* 31 (1971) 183.
- [3] C.P. Andrieux, D. Garreau, P. Hapiot, J. Pinson, J.-M. Savéant, *J. Electroanal. Chem.* 243 (1988) 321.
- [4] C.P. Andrieux, P. Hapiot, J.-M. Savéant, *Electroanalysis* 2 (1990) 183.
- [5] D.O. Wipf, E.W. Kristensen, M.R. Deakin, R.M. Wightman, *Anal. Chem.* 60 (1988) 306.
- [6] L.K. Safford, M.J. Weaver, *J. Electroanal. Chem.* 261 (1989) 241.
- [7] M. Orlik, *J. Electroanal. Chem.* 434 (1997) 139.
- [8] Z.-X. Deng, X.-Q. Lin, *J. Electroanal. Chem.* 464 (1999) 215.
- [9] J. Rosenmund, K. Doblhofer, *J. Electroanal. Chem.* 396 (1995) 77.
- [10] L. Kišova, G. Gritzner, *J. Electroanal. Chem.* 428 (1997) 73.
- [11] F. Murauer, L. Kišova, J. Komenda, G. Gritzner, *J. Electroanal. Chem.* 470 (1999) 1.
- [12] G. Fuchs, L. Kišova, J. Komenda, G. Gritzner, *J. Electroanal. Chem.* 526 (2002) 107.
- [13] L. Kišova, J. Komenda, I. Mayr, M. Orlik, G. Gritzner, *J. Electroanal. Chem.* 565 (2004) 367.
- [14] M. Orlik, *Polish J. Chem.* 72 (1998) 2272.
- [15] R. Jurczakowski, M. Orlik, *J. Electroanal. Chem.* 486 (2000) 65.
- [16] R. Jurczakowski, M. Orlik, *J. Phys. Chem. B* 106 (2002) 1058.
- [17] S.W. Feldberg, in: A.J. Bard (Ed.), *Electroanalytical Chemistry*, vol. 3, Marcel Dekker, New York, 1969, p. 199.
- [18] G.K. Kristiansen, *BIT* 3 (1963) 205.
- [19] Z. Galus, *Fundamentals of Electrochemical Analysis*, 2nd edn., Ellis Horwood/PWN, Warsaw, 1994.
- [20] A.J. Bard, L.R. Faulkner, *Electrochemical Methods: Fundamentals and Applications*, second ed., Wiley, New York, 2001.
- [21] M. Orlik, G. Gritzner, *J. Electroanal. Chem.* 421 (1997) 121.
- [22] M. Rudolph, in: I. Rubinstein (Ed.), *Physical Electrochemistry: Principles, Methods, and Applications*, Marcel Dekker, New York, 1995, p. 81.
- [23] B. Speiser, in: I. Rubinstein (Ed.), *Electroanalytical Chemistry: A Series of Advances*, vol. 19, Marcel Dekker, New York, 1996, p. 2.
- [24] M. Orlik, K. Doblhofer, G. Ertl, *J. Phys. Chem. B* 102 (1998) 6367.
- [25] M. Orlik, *J. Phys. Chem. B* 103 (1999) 6629.